
ISSN 0094-114X
ELSEVIER
Vol. 42 No. 2
February 2007
Mechanism and Machine Theory
Design Theory and Methodology
Haptics and Human-Machine-Interfaces
Robotics, Mechatronics and Micro-Machines
Mechanisms, Mechanical Transmissions and Machines
Kinematics, Dynamics and Control of Mechanical Systems
Applications to Bioengineering and Molecular Chemistry
IFToMM
Available online at
ScienceDirect
www.sciencedirect.com

Available online at www.sciencedirect.com
ScienceDirect
Mechanism and Machine Theory 42 (2007) 216–232
Mechanism and Machine Theory
www.elsevier.com/locate/mechmt

Balancing of four-bar linkages using maximum recursive dynamic algorithm

Himanshu Chaudhary *, Subir Kumar Saha

Department of Mechanical Engineering, Indian Institute of Technology Delhi, Hauz Khas, New Delhi 110 016, India

Received 19 August 2005; received in revised form 5 February 2006; accepted 28 February 2006
Available online 3 May 2006

Abstract

This paper presents a simple, computationally efficient technique for the optimum balancing of four-bar linkages. The methodology is based on the maximum recursiveness of the dynamic equations for the evaluation of bearing forces. Besides, the balancing problem is posed as an optimum problem for which the optimality criteria and the constraints are formulated. Mass distribution of linkage is embedded in the constraints to obtain physically feasible linkage. The formulation is very generic and can be easily extended to multi-loop as well.

Keywords: Optimum; Balancing; Linkage; Recursive; Dynamics

1. Introduction

The linkage balancing problem is an old problem (1) to reduce amplitude of vibration of the frame due to shaking forces and moments which in turn cause noise, wear, fatigue, etc.; and (2) to smoothen highly fluctuating input-torque needed to obtain nearly constant drive speed. However, the problem has faced new challenges, particularly, in balancing the combined shaking forces, shaking moments, and input-torque fluctuations in the design of high-speed machinery. The methods of balancing linkages are well developed and documented [1–18]. Most of the techniques are based on mass redistribution [1,2,13,14], addition of counterweights to the moving links [15,16], and attachment of rotating disks or duplication of the linkages [18]. These methods have dealt with forces involved, or the momentum fluctuations [10,11] in the linkages. Some have included bearing reactions [4] and the input-torque fluctuations [3,6,7] as well. Only few included the shaking force, the shaking moment, and the input-torque [8,13,14] in the optimality criteria. The reason could be, perhaps, as Lee and Cheng [13] have pointed out, that the nature of the problem is not simple. To name few difficulties of the linkage balancing problem,

* Corresponding author. Tel.: +91 11 26591135; fax: +91 11 26582053.
E-mail addresses: himanshubhl@rediffmail.com (H. Chaudhary), saha@mech.iitd.ernet.in (S.K. Saha).

0094-114X/$ - see front matter
doi:10.1016/j.mechmachtheory.2006.02.008

Nomenclature

$\mathbf{a}_i$	the vector representing the ith link length, and a_i the magnitude of vector $\mathbf{a}_i$ (Fig. 1)
$\bar{\mathbf{a}}_i$	$\mathbf{a}_i/a_1$, normalized vector associated to link i
$\mathbf{b}_i$	the vector from the designated joint to the application point of the working force on the ith link
$\bar{\mathbf{b}}_i$	$\mathbf{b}_i/a_1$, normalized vector of $\mathbf{b}_i$
C_i	mass centre location of the ith link
$\mathbf{d}_i$	the vector from the designated joint to the centre of mass of the ith link
$\bar{d}_{ij}$	l_{ij}/a_1, normalized distance to m_{ij}
$\mathbf{f}_i^e$	the vector of working forces applied on the ith link
$\mathbf{f}_{ij}$	the vector of force exerted on the jth link by the ith one
$\bar{\mathbf{f}}$	$\mathbf{f}/[(m_{11}+m_{12})a_1\omega_1^2]$, definition of normalized force to any force, $\mathbf{f}$
$\bar{\mathbf{f}}_i^*$	normalized inertia force of the ith link at its origin, O_i
$\bar{\mathbf{f}}_{sh}$	normalized shaking force
I_i^c	moment of inertia of the ith link about the axis perpendicular to the plane of motion at its mass centre, C_i
I_i	moment of inertia of the ith link about the axis perpendicular to plane of motion at its origin, O_i
$\bar{I}_i$	$\bar{m}_{i1}\bar{d}_{i1}^2+\bar{m}_{i2}\bar{d}_{i2}^2$, normalized moment of inertia of the ith link with respect to its origin, O_i
$\boldsymbol{l}_{ij}$	the vector from the designated joint to the equivalent mass m_{ij}
l_{ij}	distance of the equivalent mass m_{ij} from the designated joint
m_{ij}	equivalent mass of the ith link. For $j=1$, it is in the direction along the link, and for $j=2$, it is in the direction perpendicular to the link (Fig. 1)
m_i	the total mass of the ith link
$\bar{m}_{ij}$	$m_{ij}/(m_{11}+m_{12})$, Normalized equivalent point mass of link i in the jth direction
$\bar{m}_{sh}$	normalized shaking moment with respect to the reference point O_1
p_{ij}	$\bar{m}_{ij}\bar{d}_{ij}$, normalized mass–distance product of the equivalent point mass
n_i^e	working torque applied on the ith link
$\bar{n}_i^e$	$n_i^e/[(m_{11}+m_{12})a_1^2\omega_1^2]$, normalized working torque applied on the ith link
$\bar{n}_i^*$	normalized inertia torque of the ith link about its origin, O_i
σ_1, σ_2	weighting factors of the optimality criterion
$\bar{\tau}_D$	normalized driving torque
α_i	angular position of the ith link, $\alpha_1=\theta_1$; $\alpha_2=\theta_1+\theta_2$; and $\alpha_3=\theta_3$
θ_i	joint angles (Fig. 2)
ω_i	angular velocity of the ith link

Bold characters denote vectors.

- formulation of dynamic problem to calculate the joint reactions and other dynamic characteristics;
- formulation of an objective function that can be used as an index of merit for the dynamic performance of a linkage;
- constraints on design variables of the problem at hand that define bounds on the space of feasible solutions.

Determination of joint reactions, i.e., the constraint forces and moments due to the presence of kinematic joints that couple the links, involves lengthy calculations such as matrix inversion or the solution of simultaneous equations. These calculations are repeated hundreds of time in an optimization code. Lee and Cheng [13] presented an optimization technique in which an integrated approach of both the Lagrangian and Newtonian formulations is used. In particular, the driving torque is first determined using the Lagrangian approach. Then, using this information, the reactions at joints are calculated using the Newtonian approach. This way direct solution of the nine equilibrium equations for a four-bar linkage is avoided. Later, Qi and

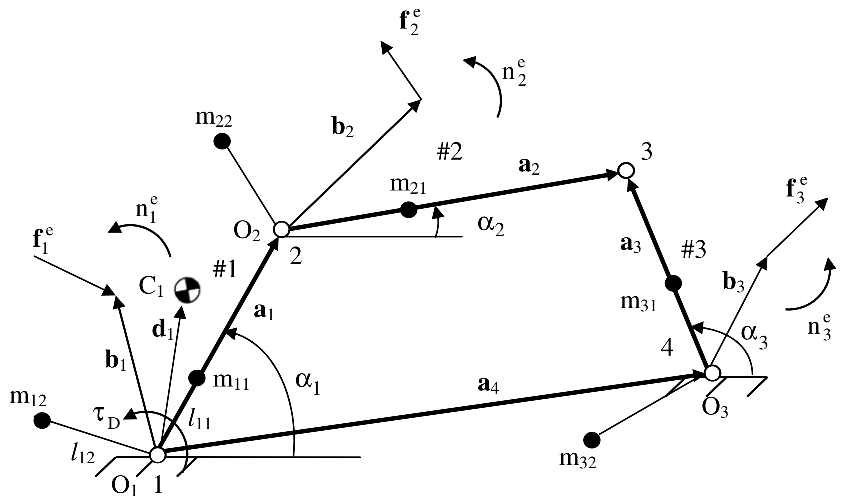

Fig. 1. An equivalent four-bar linkage using two point model.

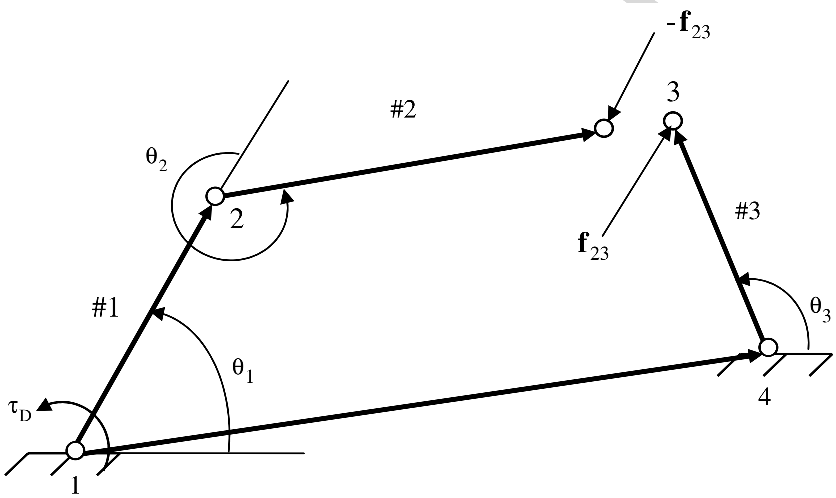

Fig. 2. Equivalent open system for the four-bar linkage.

Pennestrí [14] refined the algorithm as an alternative method for the dynamic analysis. They solved link dynamic equations in a shoe string fashion using the Newton's equations and the principle of virtual work. Still, it is required to solve four of equations simultaneously. However, using above mentioned formulations, it is difficult to obtain an analytical formulation for the linkages having more than four links. Moreover, Yan and Soong [19] have included variable input speed in the optimization scheme.

In this paper, an alternate dynamic analysis for the optimum balancing of linkages is proposed that is simple and efficient. It can be easily extended for the linkages having more than four links, and to spatial mechanisms. We use multibody dynamics approach to derive the dynamic equations. In particular, the maximum of three dynamic equations need to be solved simultaneously. Moreover, the two-point mass model [1,10] is adopted for the modelling of link inertial properties. The second part of this paper focuses on the optimality criteria and the constraints on optimizing parameters. The optimality criterion to evaluate the dynamic responses of linkages, as proposed by Lee and Cheng [13], is used here. To ensure positive moment of inertia of the links, a new constraint is introduced. In its absence, the optimization may lead to impractical solution that is not corresponding to real linkages. The optimization tool box of MATLAB software [24] is used to find the optimum design parameters of a four-bar linkage.

The paper is organised as follows: Section 2 explains the formulation for determining the shaking force and the shaking moment. An optimality criterion and constraints on optimization parameters are proposed in

Section 3. The balancing of linkages problem is then addressed as an optimization problem in Section 4, where a numerical example is presented. Conclusions are given in Section 5. The derivation of kinematic constraints and the dynamic equations associated with the four-bar linkage is given separately, in Appendix A, whereas the concept of dynamically equivalent system is presented in Appendix B.

2. Dynamic equations

In this section, a novel dynamic formulation for linkages is presented for the determination of constraint forces and moments at the joints. Based on this analytical matrix formulation, the balancing problem is posed as an optimization problem. The four-bar linkage is chosen to illustrate this approach. First, closed-loop linkage is opened by virtually cutting the joints of the independent closed loops [30,31]. For example, a four-bar linkage has only one closed-loop, and is opened by virtually cutting a joint. One can cut any of the four joints of the four-bar linkage. Then, the uncoupled Newton–Euler equations of motion for the resulting open system are written from the free-body diagrams in the Cartesian coordinates. Sequentially, the decoupled form of the natural orthogonal complement (NOC) [21] matrix associated to the open system, namely, the decoupled natural orthogonal complement matrices [20], is used to reduce the dimension of the equations of motion. This leads to a set of linear equations in terms of the constraint forces of the cut joint plus the driving torque for known motion of a mechanism. The number of constrained equations of motion depends on the number of unknown forces and moments associated with the cut-joints and driving forces/torques in the opened system. These constrained equations are solved first for the unknown forces and moments associated with the cut-joints and driving forces/torques. Since equations are linear in the cut-joint forces and moments, they can be solved using Gaussian elimination method or other efficiently [27]. Knowing the constraint forces at the cut joint, constraint forces at other joints can be determined recursively from the end body to the first body fixed to the base [25]. For a planar four-bar linkage, the constraint forces and moments are evaluated recursively with order 3 computations—3 being the number of constraint forces and moments—rather than simultaneously. Simultaneous evaluation requires the solution of nine equations with order 9^3 computations, where the number of unknowns, 9, is the size of the associated square matrix.

Note that the performance of a linkage can be predicted if the position of the mass centre, the magnitude of the mass, the principal moments of inertia, and the directions of principal axes of inertia are known for each link [1]. It is, however, often more convenient to use a dynamically equivalent system of mass points. A set of dynamically equivalent point-masses for both planar and spatial mechanisms is discussed in Appendix B. Here, the dynamically equivalent set of two point-masses [1,10] is used for the planar links motions. If the two point masses, m_{i1} and m_{i2}, are placed at distances, l_{i1} and l_{i2}, respectively, as shown in Fig. 1, the following conditions need to be satisfied:

$$m_{i1} + m_{i2} = m_i \tag{1a}$$

$$m_{i1}\boldsymbol{l}_{i1} + m_{i2}\boldsymbol{l}_{i2} = m_i\mathbf{d}_i \tag{1b}$$

$$m_{i1}l_{i1}^2 + m_{i2}l_{i2}^2 = I_i^c + m_i d_i^2 \tag{1c}$$

Eqs. (1a–c) provides four scalar equations in four unknowns, m_{i1}, m_{i2}, l_{i1} and l_{i2}. For the given link mass, m_i, its mass centre location, $\mathbf{d}_i$, and the mass moment of inertia, I_i^c, one can then find the dynamic equivalent system comprising two point masses. Next, the four-bar linkage, Fig. 1, is opened by cutting joint 3. In order to maintain the equilibrium, reaction forces at the cut joint 3, $\mathbf{f}_{23}$, are introduced in the open system. The Newton–Euler (NE) equations of motion for the ith rigid link are then written as follows: Referring to Eq. (A.15)

$$\mathbf{M}_i\dot{\mathbf{t}}_i + \mathbf{C}_i\mathbf{t}_i = \mathbf{w}_i \tag{2}$$

where the 3×3 matrices, $\mathbf{M}_i$ and $\mathbf{C}_i$ are defined as

$$\mathbf{M}_i \equiv \begin{bmatrix} I_i & -m_i\mathbf{d}_i^T\mathbf{E} \\ m_i\mathbf{E}\mathbf{d}_i & m_i\mathbf{1} \end{bmatrix} \text{ and } \mathbf{C}_i \equiv \begin{bmatrix} 0 & \mathbf{0}^T \\ -m_i\omega_i\mathbf{d}_i & \mathbf{O} \end{bmatrix} \tag{3}$$

Moreover, the three-dimensional vectors, $\mathbf{t}_i$ and $\mathbf{w}_i$ are defined in Eqs. (A.1) and (A.8), respectively. Furthermore, m_i, I_i, $\mathbf{d}_i$, and ω_i are defined in the nomenclature. Using the dynamic equivalent system of point masses, Eq. (1), the $\mathbf{M}_i$ and $\mathbf{C}_i$ are obtained as

$$\mathbf{M}_i \equiv \begin{bmatrix} m_{i1}l_{i1}^2 + m_{i2}l_{i2}^2 & -(m_{i1}l_{i1}s\alpha_i + m_{i2}l_{i2}c\alpha_i) & m_{i1}l_{i1}c\alpha_i - m_{i2}l_{i2}s\alpha_i \\ -(m_{i1}l_{i1}s\alpha_i + m_{i2}l_{i2}c\alpha_i) & m_{i1} + m_{i2} & 0 \\ m_{i1}l_{i1}c\alpha_i - m_{i2}l_{i2}s\alpha_i & 0 & m_{i1} + m_{i2} \end{bmatrix}$$

and

$$\mathbf{C}_i \equiv \begin{bmatrix} 0 & 0 & 0 \\ -\ \omega_i(m_{i1}l_{i1}c\alpha_i - m_{i2}l_{i2}s\alpha_i) & 0 & 0 \\ -\omega_i(m_{i1}l_{i1}s\alpha_i + m_{i2}l_{i2}c\alpha_i) & 0 & 0 \end{bmatrix} \tag{4}$$

where m_{ij}, l_{ij}, and α_i are defined in the nomenclature and shown in Fig. 1. Furthermore, $s\alpha_i \equiv \sin\alpha_i$ and $c\alpha_i \equiv \cos\alpha_i$. Since there are quantities of different units, e.g., reactions forces, driving torque, etc. the elements of the vectors and matrices of Eq. (2) are normalized. Corresponding to the Euler equation of rotation motion, i.e., the first scalar equation of Eq. (2), and the Newton equations, i.e., the second and third scalar equations of Eq. (2), the normalized factors are, $(m_{11} + m_{12})a_1^2\omega_1^2$ and $(m_{11} + m_{12})a_1\omega_1^2$, respectively, which lead to the modified expressions for Eq. (2), i.e.,

$$\overline{\mathbf{M}}_\mathbf{i}\dot{\bar{\mathbf{t}}}_\mathbf{i} + \bar{\mathbf{C}}_\mathbf{i}\bar{\mathbf{t}}_\mathbf{i} = \bar{\mathbf{w}}_\mathbf{i} \tag{5}$$

where

$$\overline{\mathbf{M}}_\mathbf{i} \equiv \begin{bmatrix} \bar{I}_i & -(p_{i1}s\alpha_i + p_{i2}c\alpha_i) & (p_{i1}c\alpha_i - p_{i2}s\alpha_i) \\ -(p_{i1}s\alpha_i + p_{i2}c\alpha_i) & (\bar{m}_{i1} + \bar{m}_{i2}) & 0 \\ (p_{i1}c\alpha_i - p_{i2}s\alpha_i) & 0 & (\bar{m}_{i1} + \bar{m}_{i2}) \end{bmatrix}$$

and

$$\bar{\mathbf{C}}_i \equiv \begin{bmatrix} 0 & 0 & 0 \\ -(p_{i1}c\alpha_i - p_{i2}s\alpha_i)\omega_i/\omega_1 & 0 & 0 \\ -(p_{i1}s\alpha_i + p_{i2}c\alpha_i)\omega_i/\omega_1 & 0 & 0 \end{bmatrix} \tag{6}$$

In Eq. (6), p_{ij} and $\bar{m}_{ij}$ are defined in the nomenclature. Moreover, the normalized twist and twist-rate are as follows:

$$\bar{\mathbf{t}} \equiv \begin{bmatrix} \omega_i/\omega_1 \\ \mathbf{v}_i/(a_1\omega_1) \end{bmatrix} \text{ and } \dot{\bar{\mathbf{t}}} \equiv \begin{bmatrix} \dot{\omega}_i/\omega_1^2 \\ \dot{\mathbf{v}}_i/(a_1\omega_1^2) \end{bmatrix} \tag{7}$$

Eq. (5) for all the three moving links of the four-bar linkage are put together as

$$\overline{\mathbf{M}}\dot{\bar{\mathbf{t}}} + \bar{\mathbf{C}}\bar{\mathbf{t}} = \bar{\mathbf{w}} \tag{8a}$$

where the 9×9 matrices, $\overline{\mathbf{M}}$ and $\bar{\mathbf{C}}$, are the generalized mass and connective inertia matrices, respectively, which are defined as

$$\overline{\mathbf{M}} \equiv \text{diag}[\overline{\mathbf{M}}_\mathbf{1}, \ldots, \overline{\mathbf{M}}_\mathbf{3}] \text{ and } \bar{\mathbf{C}} \equiv \text{diag}[\bar{\mathbf{C}}_\mathbf{1}, \ldots, \bar{\mathbf{C}}_\mathbf{3}] \tag{8b}$$

In Eq. (8a), the nine-dimensional vectors of normalized twist-rate and wrench, $\dot{\bar{\mathbf{t}}}$ and $\bar{\mathbf{w}}$, respectively, are as follows:

$$\dot{\bar{\mathbf{t}}} \equiv \left[\dot{\bar{\mathbf{t}}}_1^{\mathrm{T}}, \cdots, \dot{\bar{\mathbf{t}}}_3^{\mathrm{T}}\right]^{\mathrm{T}} \text{ and } \bar{\mathbf{w}} \equiv \left[\bar{\mathbf{w}}_1^{\mathrm{T}}, \cdots, \bar{\mathbf{w}}_3^{\mathrm{T}}\right]^{\mathrm{T}} \tag{8c}$$

Eq. (8a) shows the uncoupled NE equations of motion of the free-bodies of the linkage. One can solve these nine equations to calculate the nine unknowns which is, in particular, computationally very costly for a general purpose optimization code. Since the constraint forces and moments do not perform any useful work

[20–23], they can be eliminated from the equations of motion. In this process the dimension of the system of equations is reduced. Here, the concept of the natural orthogonal complement (NOC) [21] is used to reduce the dimension of equations. Premultiplying Eq. (8a) with the transpose of the NOC results

$$\overline{\mathbf{N}}^{\mathrm{T}}(\overline{\mathbf{M}}\dot{\bar{\mathbf{t}}} + \bar{\mathbf{C}}\bar{\mathbf{t}}) = \overline{\mathbf{N}}^{\mathrm{T}}\bar{\mathbf{w}} \tag{9}$$

In Eq. (9), $\overline{\mathbf{N}}$ is the 9×3 normalized NOC in line with the normalized NE equations of motion, Eq. (8a), which is different than the original definition of the NOC, as proposed in [21] and derived in [26]. If the normalized wrench due to all the constraint forces and moments, i.e., the reactions, is denoted by $\bar{\mathbf{w}}^{\mathrm{R}}$, and the normalized wrench due to all the external or working forces and moments, is denoted by, $\bar{\mathbf{w}}^{\mathrm{E}}$, then, $\bar{\mathbf{w}} = \bar{\mathbf{w}}^{\mathrm{R}} + \bar{\mathbf{w}}^{\mathrm{E}}$. Rewriting Eq. (9)

$$\overline{\mathbf{N}}^{\mathrm{T}}(\overline{\mathbf{M}}\dot{\bar{\mathbf{t}}} + \bar{\mathbf{C}}\bar{\mathbf{t}}) = \overline{\mathbf{N}}^{\mathrm{T}}(\bar{\mathbf{w}}^{\mathrm{R}} + \bar{\mathbf{w}}^{\mathrm{E}}) \tag{10}$$

and denoting, $\bar{\boldsymbol{\tau}}^{\mathrm{R}} \equiv \overline{\mathbf{N}}^{\mathrm{T}}\bar{\mathbf{w}}^{\mathrm{R}}$ and $\bar{\boldsymbol{\tau}}^{\mathrm{E}} \equiv \overline{\mathbf{N}}^{\mathrm{T}}\bar{\mathbf{w}}^{\mathrm{E}}$, Eq. (10) is rewritten as

$$\overline{\mathbf{N}}^{\mathrm{T}}(\overline{\mathbf{M}}\dot{\bar{\mathbf{t}}} + \bar{\mathbf{C}}\bar{\mathbf{t}}) = \bar{\boldsymbol{\tau}}^{\mathrm{R}} + \bar{\boldsymbol{\tau}}^{\mathrm{E}} \tag{11}$$

where the expression for the normalized natural orthogonal complement matrix, $\overline{\mathbf{N}}$, is derived from the definition of the decoupled natural orthogonal complement matrices, i.e., Eq. (A.7). The normalized form, $\overline{\mathbf{N}}$, is given by

$$\overline{\mathbf{N}} \equiv \begin{bmatrix} \mathbf{p}_1 & \mathbf{0} & \mathbf{0} \\ \bar{\mathbf{A}}_{21}\mathbf{p}_1 & \mathbf{p}_2 & \mathbf{0} \\ \mathbf{0} & \mathbf{0} & \mathbf{p}_3 \end{bmatrix} \tag{12}$$

whereas the generalized constraint forces and moments, $\bar{\boldsymbol{\tau}}^{\mathrm{R}}$, are obtained as

$$\bar{\boldsymbol{\tau}}^{\mathrm{R}} = \begin{bmatrix} 1 & (\bar{\mathbf{a}}_1 + \bar{\mathbf{a}}_2)^{\mathrm{T}}\mathbf{E} \\ 0 & \bar{\mathbf{a}}_2^{\mathrm{T}}\mathbf{E} \\ 0 & -\bar{\mathbf{a}}_3^{\mathrm{T}}\mathbf{E} \end{bmatrix} \begin{bmatrix} \bar{\tau}_{\mathrm{D}} \\ \bar{\mathbf{f}}_{23} \end{bmatrix} \tag{13}$$

In which the following expressions for the constraint wrenches of the links are used:

$$\bar{\mathbf{w}}_1^{\mathrm{R}} \equiv \begin{bmatrix} \bar{\tau}_{\mathrm{D}} + \bar{\mathbf{a}}_1^{\mathrm{T}}\mathbf{E}\bar{\mathbf{f}}_{12} \\ \bar{\mathbf{f}}_{41} - \bar{\mathbf{f}}_{12} \end{bmatrix}; \quad \bar{\mathbf{w}}_2^{\mathrm{R}} \equiv \begin{bmatrix} \bar{\mathbf{a}}_2^{\mathrm{T}}\mathbf{E}\bar{\mathbf{f}}_{23} \\ \bar{\mathbf{f}}_{12} - \bar{\mathbf{f}}_{23} \end{bmatrix}; \text{ and } \bar{\mathbf{w}}_3^{\mathrm{R}} \equiv \begin{bmatrix} -\bar{\mathbf{a}}_3^{\mathrm{T}}\mathbf{E}\bar{\mathbf{f}}_{23} \\ \bar{\mathbf{f}}_{23} - \bar{\mathbf{f}}_{34} \end{bmatrix} \tag{14}$$

Note that the driving torque is taken as a constraint torque because it is constraining the input motion. In Eq. (12), the three-dimensional joint-rate propagation vectors, $\mathbf{p}_i$, $i = 1$, 2, and 3, are defined in Eq. (A.4) and the 3×3 twist propagation matrix, $\bar{\mathbf{A}}_{21}$, is obtained using Eq. (A.3), i.e.,

$$\bar{\mathbf{A}}_{21} \equiv \begin{bmatrix} 1 & \mathbf{0}^{\mathrm{T}} \\ \mathbf{E}\bar{\mathbf{a}}_1 & \mathbf{1} \end{bmatrix} \tag{15}$$

Moreover, the normalized NOC, $\overline{\mathbf{N}}$, is derived for the open system obtained from cutting the joint, 3, of the four-bar linkage. Here, the constraint forces, $\bar{\mathbf{f}}_{23}$, appear in Eq. (13). Other, reactions acting at joints, 1, 2, and 4, i.e., $\bar{\mathbf{f}}_{41}$, $\bar{\mathbf{f}}_{12}$, and $\bar{\mathbf{f}}_{34}$, are eliminated from Eq. (11) [20,21] using the NOC. Furthermore, the wrenches due to external forces and moments are expressed as follows:

$$\bar{\mathbf{w}}_i^{\mathrm{E}} \equiv \begin{bmatrix} 1 & -\bar{\mathbf{b}}_i^{\mathrm{T}}\mathbf{E} \\ O & \mathbf{1} \end{bmatrix} \begin{bmatrix} \bar{n}_i^{\mathrm{e}} \\ \bar{\mathbf{f}}_i^{\mathrm{e}} \end{bmatrix} \text{ for } i = 1, 2, 3 \tag{16}$$

Using Eq. (16), the generalized forces, i.e., the torques due to external forces and moments, $\bar{\tau}^{\mathrm{E}}$, are determined as

$$\bar{\boldsymbol{\tau}}^{\mathrm{E}} = \begin{bmatrix} \bar{n}_1^{\mathrm{e}} - \bar{\mathbf{b}}_1^{\mathrm{T}}\mathbf{E}\bar{\mathbf{f}}_1^{\mathrm{e}} + \bar{n}_2^{\mathrm{e}} - \bar{\mathbf{b}}_2^{\mathrm{T}}\mathbf{E}\bar{\mathbf{f}}_2^{\mathrm{e}} - \bar{\mathbf{a}}_1^{\mathrm{T}}\mathbf{E}\bar{\mathbf{f}}_2^{\mathrm{e}} \\ \bar{n}_2^{\mathrm{e}} - \bar{\mathbf{b}}_2^{\mathrm{T}}\mathbf{E}\bar{\mathbf{f}}_2^{\mathrm{e}} \\ n_3^{\mathrm{e}} - \bar{\mathbf{b}}_3^{\mathrm{T}}\mathbf{E}\bar{\mathbf{f}}_3^{\mathrm{e}} \end{bmatrix} \tag{17}$$

Denoting the expression on the left hand side of Eq. (5) as $\mathbf{w}_i^*$, which defined as the three-dimensional inertia wrench, i.e., $\mathbf{w}_i^* \equiv [\bar{n}_i^*, \bar{\mathbf{f}}_i^{*\mathrm{T}}]^{\mathrm{T}}$, and substituting Eqs. (13) and (17) into Eq. (11), one obtains

$$\begin{bmatrix} \bar{n}_1^* + \bar{n}_2^* - \bar{\mathbf{a}}_1^{\mathrm{T}}\mathbf{E}\bar{\mathbf{f}}_2^* \\ \bar{n}_2^* \\ \bar{n}_3^* \end{bmatrix} = \begin{bmatrix} 1 & (\bar{\mathbf{a}}_1 + \bar{\mathbf{a}}_2)^{\mathrm{T}}\mathbf{E} \\ 0 & \bar{\mathbf{a}}_2^{\mathrm{T}}\mathbf{E} \\ 0 & -\bar{\mathbf{a}}_3^{\mathrm{T}}\mathbf{E} \end{bmatrix} \begin{bmatrix} \bar{\tau}_{\mathrm{D}} \\ \bar{\mathbf{f}}_{23} \end{bmatrix} + \begin{bmatrix} \bar{n}_1^{\mathrm{e}} - \bar{\mathbf{b}}_1^{\mathrm{T}}\mathbf{E}\bar{\mathbf{f}}_1^{\mathrm{e}} + \bar{n}_2^{\mathrm{e}} - \bar{\mathbf{b}}_2^{\mathrm{T}}\mathbf{E}\bar{\mathbf{f}}_2^{\mathrm{e}} - \bar{\mathbf{a}}_1^{\mathrm{T}}\mathbf{E}\bar{\mathbf{f}}_2^{\mathrm{e}} \\ \bar{n}_2^{\mathrm{e}} - \bar{\mathbf{b}}_2^{\mathrm{T}}\mathbf{E}\bar{\mathbf{f}}_2^{\mathrm{e}} \\ \bar{n}_3^{\mathrm{e}} - \bar{\mathbf{b}}_3^{\mathrm{T}}\mathbf{E}\bar{\mathbf{f}}_3^{\mathrm{e}} \end{bmatrix} \tag{18}$$

Eq. (18) is now linear in a smaller set of unknowns, i.e., the constraint forces at the cut joint, $\bar{\mathbf{f}}_{23}$, and the driving torque, $\bar{\tau}_{\mathrm{D}}$. Here, one needs to solve only three scalar equations simultaneously instead of nine in the traditional approach. The remaining normalized reactions are then determined recursively using the force and moment balance equations [25], namely,

$$\bar{\mathbf{w}}_{i-1,i} = \overline{\mathbf{A}'}_{i,i+1}\bar{\mathbf{w}}_{i,i+1} + \bar{\mathbf{w}}_i^* - \bar{\mathbf{w}}_i^{\mathrm{E}} \tag{19}$$

where the three-dimensional vectors, $\bar{\mathbf{w}}_{i-1,i}$ and $\bar{\mathbf{w}}_{i,i+1}$, are defined as the constraint wrenches at the joints between links, #$(i-1)$ and #i, and #i and #$(i+1)$, respectively, i.e.,

$$\bar{\mathbf{w}}_{i-1,i} \equiv \begin{bmatrix} \bar{n}_{i,i-1} \\ \bar{\mathbf{f}}_{i,i-1} \end{bmatrix} \text{ and } \bar{\mathbf{w}}_{i,i+1} \equiv \begin{bmatrix} \bar{n}_{i,i+1} \\ \bar{\mathbf{f}}_{i,i+1} \end{bmatrix} \tag{20}$$

Moreover, the 3×3 matrix, $\mathbf{A}'_{i,i+1} = \mathbf{A}^{\mathrm{T}}_{i+1,i}$—$\mathbf{A}_{i,i+1}$ being defined similar to $\mathbf{A}_{ij}$ of Eq. (A.3). Furthermore, $\bar{\mathbf{w}}_i^{\mathrm{E}}$ is obtained similar to Eq. (16). Once all the joint reactions are determined one can calculate the shaking force and the shaking moment as

$$\bar{\mathbf{f}}_{\mathrm{sh}} = -(\bar{\mathbf{f}}_{41} + \bar{\mathbf{f}}_{43} + \bar{\mathbf{f}}_1^{\mathrm{e}} + \bar{\mathbf{f}}_2^{\mathrm{e}} + \bar{\mathbf{f}}_3^{\mathrm{e}}) \tag{21}$$

$$\bar{m}_{\mathrm{sh}} = -[\bar{\tau}_{\mathrm{D}} + \bar{n}_1^{\mathrm{e}} + \bar{n}_2^{\mathrm{e}} + \bar{n}_3^{\mathrm{e}} - \bar{\mathbf{a}}_4^{\mathrm{T}}\mathbf{E}\bar{\mathbf{f}}_{43} - \bar{\mathbf{b}}_1^{\mathrm{T}}\mathbf{E}\bar{\mathbf{f}}_1^{\mathrm{e}} - (\bar{\mathbf{a}}_1 + \bar{\mathbf{b}}_2)^{\mathrm{T}}\mathbf{E}\bar{\mathbf{f}}_2^{\mathrm{e}} - (\bar{\mathbf{a}}_4 + \bar{\mathbf{b}}_3)^{\mathrm{T}}\mathbf{E}\bar{\mathbf{f}}_3^{\mathrm{e}}] \tag{22}$$

where normalized shaking moment, $\bar{m}_{\mathrm{sh}}$, is obtained with respect to point O_1.

Since the focus of this paper is on planar four-bar linkage, equations are derived systematically for the four-linkage. However, for the spatial linkages the dynamic equations are given in Eq. (A.17) [25,26]. The inertial properties of links of a spatial linkage can be derived in terms of equimomental point masses using Eqs. (B.5)–(B.14). For the multiloop systems, similar treatment can be done; where the number of joints to be cut is equal to the number of independent loops exist in a mechanism. The results of the multiloop systems were also obtained, which are not reported here, as the emphasis of this paper is to show the formulation of the problem in a closed-loop system.

3. An optimality criteria and constraints

Dynamical performance of a four-bar linkage is evaluated by a function which is a linear combination of the resultant bearing force on the supporting frame, and the input-torque required to drive the linkage [13,14]. Such function is called the objective function, s, which is to be minimized. It is expressed as

$$s = \frac{1}{T}\int_0^{\mathrm{T}} \left(\sigma_1\sqrt{\bar{f}_{14}^2 + \bar{f}_{34}^2} + \sigma_2\sqrt{\bar{\tau}_{\mathrm{D}}^2}\right)\mathrm{d}t \tag{23}$$

where $\bar{\mathbf{f}}_{14}$ and $\bar{\mathbf{f}}_{34}$ denote the magnitudes of the dimensionless bearing forces on the frame through joints 1 and 4, i.e., $\bar{\mathbf{f}}_{14}$ and $\bar{\mathbf{f}}_{34}$, respectively; and σ_1 and σ_2 are the weighting factors. Based on the dynamic analysis presented in Section 2, nine parameters appearing in Eq. (6), namely, p_{ij} and $\bar{I}_i$, for $i = 1, 2, 3; j = 1, 2$, are chosen as the optimizing parameters. These parameters are the inertial properties of the linkage, as explained in Section 2. Hence, the term, s, is a function of these nine parameters. The proper selection of these parameters leads to a minimum value of the function, s. Hence, the linkage balancing problem is formulated as an optimization problem. In this paper, the balancing of the linkages is considered through the redistribution of the link masses, whereas the constraints could be the space requirement, amplitude of the input-torque fluctuation, magnitude of the bearing forces, etc. In addition, the optimizing parameters are constrained in a way that the moment of inertia of any link must not be zero. Such constraint can be obtained from Eq. (1) as

$$\bar{I}_i - \frac{m_1}{m_i}p_{i1}^2 - \frac{m_1}{m_i}p_{i2}^2 = \frac{I_i^c}{m_1 a_1^2} \quad (24)$$

which can be restated by substituting $I_i^c \equiv m_i k_i^2$—k_i being the radius of gyration as

$$\frac{m_i}{m_1}(k_{i,\min}/a_1)^2 \leqslant \bar{I}_i - \frac{m_1}{m_i}p_{i1}^2 - \frac{m_1}{m_i}p_{i2}^2 \leqslant \frac{m_i}{m_1}(k_{i,\max}/a_1)^2 \quad (25)$$

Moreover, $k_{i,\min}$ and $k_{i,\max}$ are the minimum and maximum bounds for $k_{i.}$ The constraints, Eq. (25), ensures non-negativity of the moment inertia of ith link, and the limits on the radius of gyration for the mass distribution.

4. Optimization problem

Based on Eqs. (23) and (25), the balancing problem is now formally posed as

$$\text{Minimize}: s = \frac{1}{T}\int_0^T \left(\sigma_1\sqrt{\bar{f}_{14}^2 + \bar{f}_{34}^2} + \sigma_2\sqrt{\bar{\tau}_{\mathrm{D}}^2}\right)\mathrm{d}t \quad (26)$$

$$\text{Subject to}: \frac{m_i}{m_1}(k_{i,\min}/a_1)^2 \leqslant \bar{I}_i - \frac{m_1}{m_i}p_{i1}^2 - \frac{m_1}{m_i}p_{i2}^2 \leqslant \frac{m_i}{m_1}(k_{i,\max}/a_1)^2 \quad (27)$$

Many optimization techniques are available in the literature. For example, Heuristic optimization technique of Lee and Cheng [13], and others [5]. In this paper the optimization tool box of MATLAB [24] is used. This tool box provides several functions based on different algorithms. The optimized results of this paper are obtained using "fmincon" function.

4.1. Numerical example

Effectiveness of the balancing method proposed in Sections 2 and 3 is compared with the balancing methods presented in Berkof and Lowen [12], and Lee and Cheng [13]. A four-bar linkage that has been optimized in the literatures [12,13] referred here as the standard four-bar linkage whose link's length proportions, masses, and the moment of inertia about the centre of gravity are given in Table 1. Its optimized parameters are given in Table 2. In order to show the effectiveness of the proposed algorithm the same linkage is optimized here. The driving torque, the shaking force and moment are obtained using the optimized values of the proposed methodology, and those reported in Berkof and Lowen [12], and Lee and Cheng [13]. Note that there is a sign mistake in one of the parameters reported by Lee and Cheng [13], and Qi and Pennestrí [14]. The parameter, p_{21} of Table 2, has a minus sign, which should be positive. All the results produced in this paper using $p_{21} = 1.16$. The comparison of the results shows a good match. Signs with plus sign the results produced here matches exactly with those of [13]. Different weighting factors and the limits on the radius of gyration are taken for the present analyses are as follows:

Table 1
Link proportions and inertial properties of the standard linkage

Link number	Link proportions (a_i/a_1)	Mass of links (kg)	Moment of inertia about centre of gravity (kg-m^2)
1	1	0.04585	0.6733×10^{-5}
2	2	0.05317	0.3013×10^{-4}
3	3	0.06602	0.6768×10^{-4}
4	3[a]	–	–

$a_1 = 0.0254$ m.
[a] In [12], it is 3.695.

Table 2
Parameters of standard linkage and balance parameters for different methods

Balancing method	p_{11}	p_{12}	p_{21}	p_{22}	p_{31}	p_{32}	$\bar{I}_1$	$\bar{I}_2$	$\bar{I}_3$
Standard linkage	0.500	0.000	1.160	0.000	2.160	0.000	0.580	2.178	5.528
Berkof and Lowen [12]	−0.580	0.000	−1.160[a]	0.000	−1.740	0.000	1.594	2.178	8.340
Lee and Cheng [13]	−1.160	−0.006	0.203	−0.406	0.615	0.441	0.812	0.928	2.320
Case-I	−1.234	0.000	0.0174	−0.075	0.243	0.128	2.411	0.295	0.862
Case-II	0.500	0.000	1.160	0.000	2.160	0.000	0.580	2.178	5.528
Case-III	−1.244	−0.002	−0.005	−0.089	0.244	0.125	2.543	0.297	0.862
Case-IV	−1.373	−0.005	0.007	−0.215	0.485	0.239	2.886	0.790	2.273
Case-V	−1.488	−0.008	0.029	−0.305	0.0590	0.288	3.214	1.241	3.539

[a] In [13], it is reported as −1.160. However, the correct value should be 1.160 as discussed in Section 4.1.

Case-I $\sigma_1 = 1.0,\ \sigma_2 = 0.0,\ k_{i,\min} = a_i/4,\ k_{i,max} = a_i$

Case-II $\sigma_1 = 0.0;\ \sigma_2 = 1.0;\ k_{i,\min} = a_i/4;\ k_{i,\max} = a_i$

Case-III $\sigma_1 = 0.5;\ \sigma_2 = 0.5;\ k_{i,\min} = a_i/4;\ k_{i,\max} = a_i$

Case-IV $\sigma_1 = 0.5;\ \sigma_2 = 0.5;\ k_{i,\min} = a_i/2.5;\ k_{i,\max} = a_i$

Case-V $\sigma_1 = 0.5;\ \sigma_2 = 0.5;\ k_{i,\min} = a_i/2;\ k_{i,\max} = a_i$

The purpose to use different weighting factors is to investigate the influence of bearing forces and driving torque on the over-all dynamic performances. Numerical values of all the balancing parameters obtained for various methods are shown in Table 2. The RMS (root mean square) values of the dynamic characteristics for the different cases are compared with the reported optimized characteristics [12,13] in Table 3. The comparison in Table 3 shows that among five cases, Case-III is optimum. For instance, the RMS value of the shaking moment shows reduction of 90% over the standard linkage, while other methods, namely, Berkof and Lowen [12], and Lee and Cheng [13], there is an increase of 72% and reduction of 77%, respectively. For the RMS driving torque, Case-III gives reduction of 94% as compared to the reduction of 13% and 80% in [12] and [13], respectively. Fig. 3 shows a comparison of the different performance parameters of the optimum linkage of this investigation, i.e., Case-III, with those reported in [12] and [13], and the standard linkage. The effect of the moment of inertia bounds on the dynamical quantities is shown in Fig. 4, which shows Linkage-III is optimum.

The comparison of Cases III–V show that the lower limits on the moment of inertia, i.e., the radius of gyration, improves the dynamic performances. Moreover, Fig. 5 shows the comparison between the quantities using different weighting factors. This also provides the optimum performance parameters for Case-III. The dynamic parameters of Case-IV are comparable to that of Lee and Cheng [13].

Table 3
RMS values of dynamic quantities of standard and balanced linkages

Balancing method	($k_{i,min}$, $k_{i,max}$)	RMS values		
		Driving torque	Shaking force	Shaking moment[a]
Standard linkage	Not available	0.8614	2.0599	2.3384
Berkof and Lowen [12]: $\sigma_1 = 0.5$; $\sigma_1 = 0.5$	Not available	0.7497 (−13)[b]	0.000 (−100)	4.0111 (72)
Lee and Cheng [13]: $\sigma_1 = 0.5$; $\sigma_1 = 0.5$	Not available	0.1693 (−80)	0.2908 (−86)	0.5344 (−77)
Case-I: $\sigma_1 = 1.0$; $\sigma_1 = 0.0$	(a_i/4, a_i)	0.0587 (−93)	0.0881 (−95)	0.2333 (−90)
Case-II: $\sigma_1 = 0.0$; $\sigma_1 = 1.0$	(a_i/4, a_i)	0.8614 (00)	2.0599 (00)	2.3384 (00)
Case-III: $\sigma_1 = 0.5$; $\sigma_1 = 0.5$	**(a_i/4, a_i)**	**0.0496 (−94)**	**0.0840 (−96)**	**0.2310 (−90)**
Case-IV: $\sigma_1 = 0.5$; $\sigma_1 = 0.5$	(a_i/2.5, a_i)	0.1413 (−83)	0.2064 (−90)	0.7296 (−69)
Case-V: $\sigma_1 = 0.5$; $\sigma_1 = 0.5$	(a_i/2, a_i)	0.2340 (−73)	0.3189 (−84)	1.2715 (−46)

[a] The shaking moment is taken with respect to the driving joint, i.e., joint 1 (Fig. 1).
[b] The values in the parenthesis denote the percentage increment/decrement over the corresponding RMS values over the standard linkage.

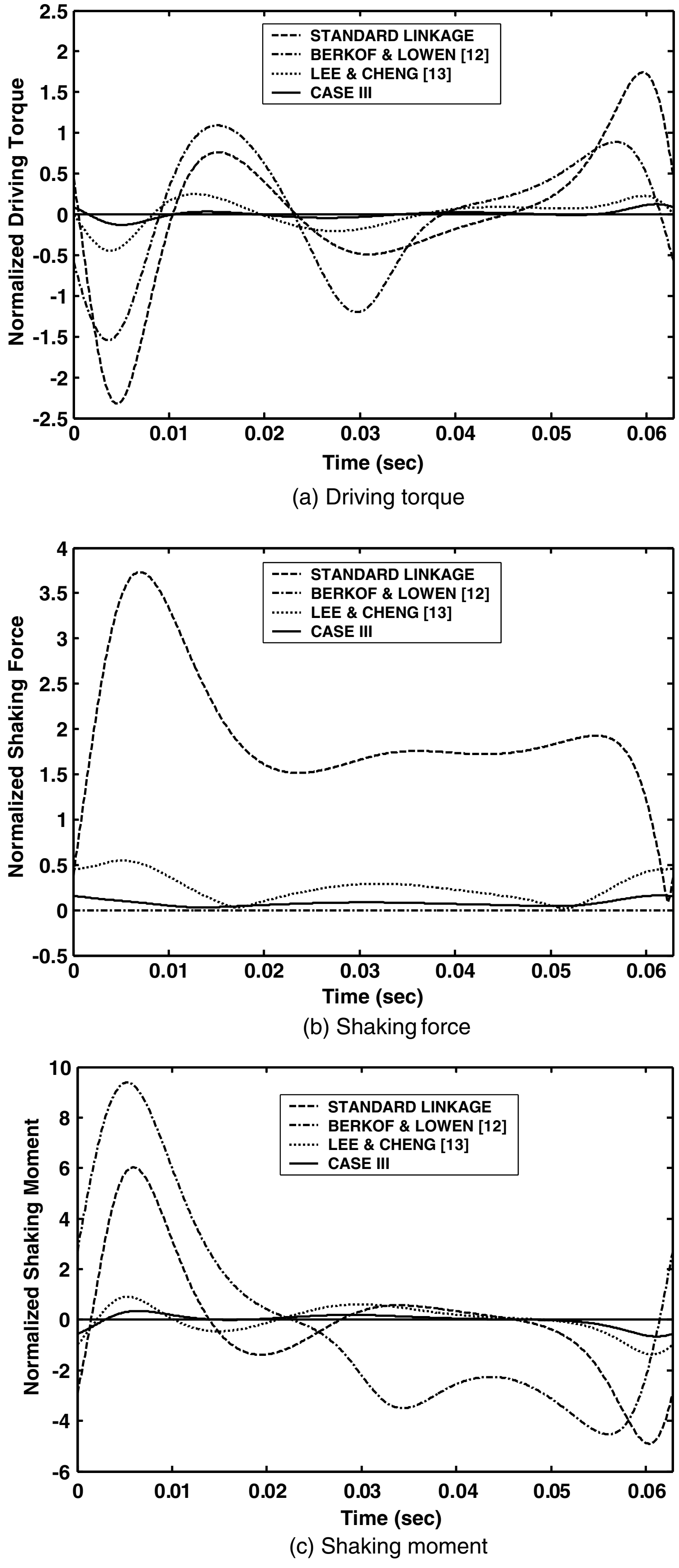

Fig. 3. Performances using different balancing methods.

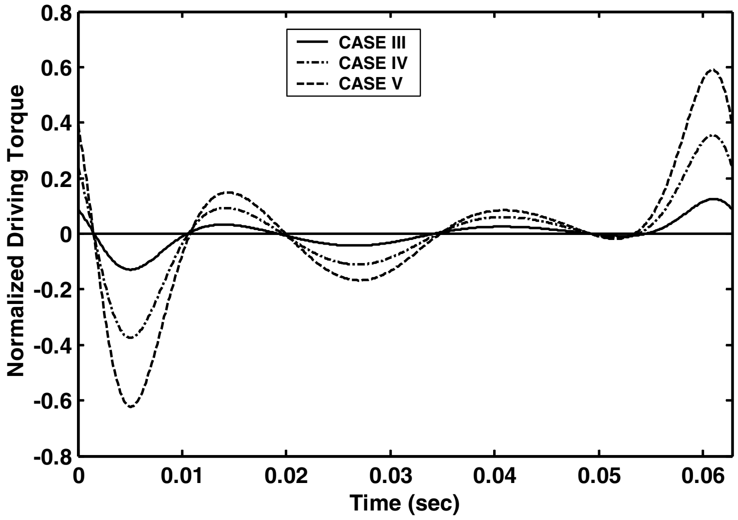

(a) Driving torque

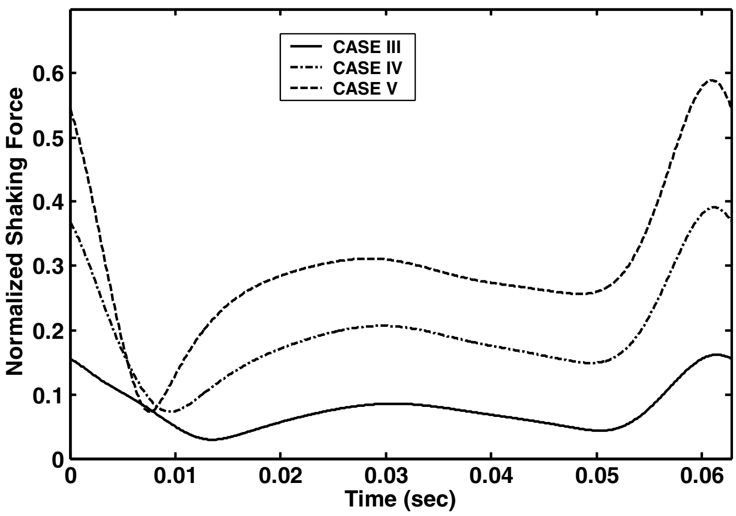

(b) Shaking force

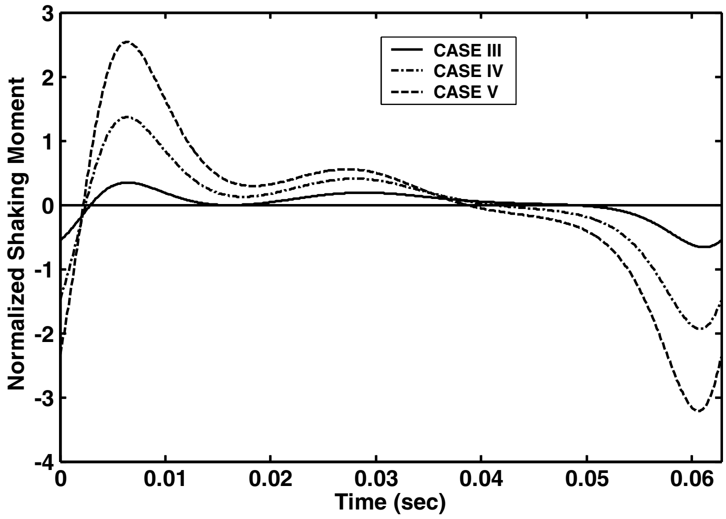

(c) Shaking moment

Fig. 4. Performances using different radius of gyration limits.

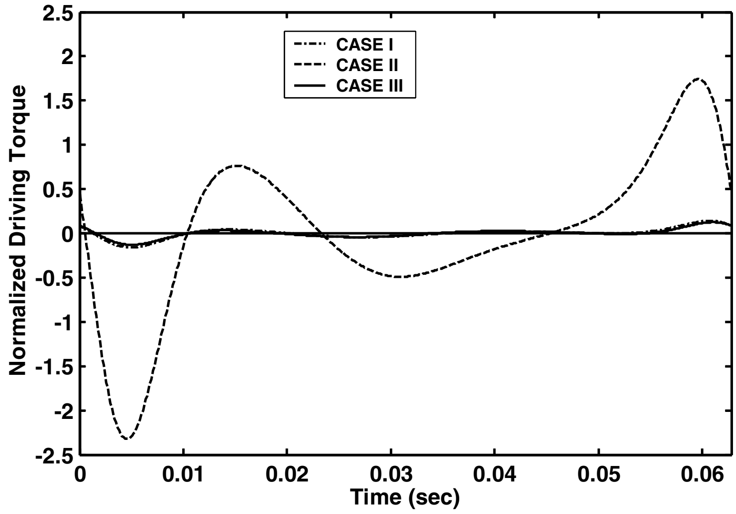

(a) Driving torque

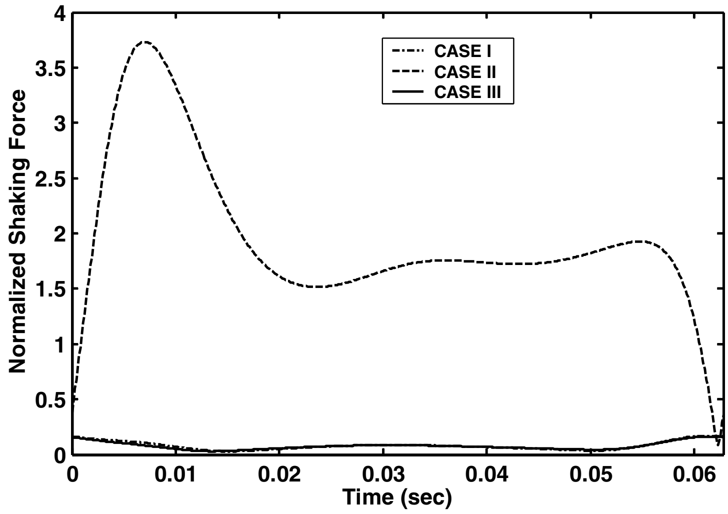

(b) Shaking force

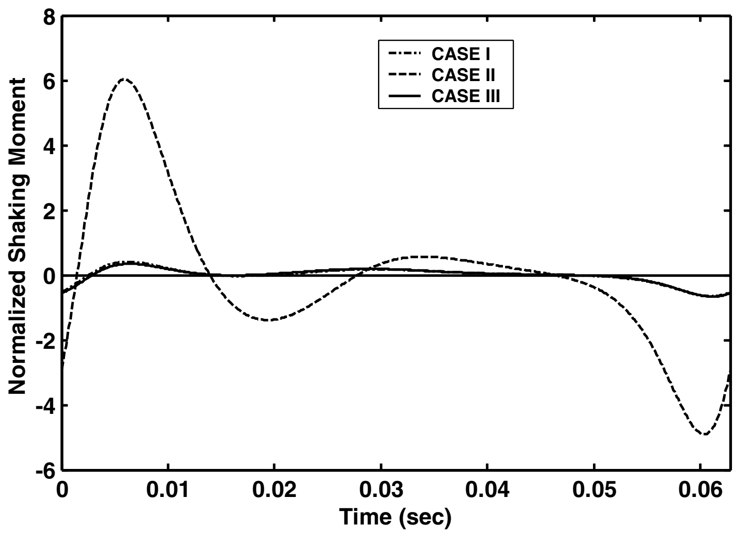

(c) Shaking moment

Fig. 5. Performance using different weight factors for same radius of gyration.

5. Conclusions

A novel simple approach for the dynamic balancing of a four-bar linkage is presented in this paper using the maximum recursive dynamic algorithm for the evaluation of the bearing forces. A maximum of three scalar equations, namely, Eq. (18), need to be solved simultaneously. Since the solution of n scalar algebraic equations takes order (n^3) computations [27] the complexity of the proposed algorithm reduces drastically (~10 times or more) in comparison of solving nine simultaneous equations. This is one of the key contributions of this paper. Besides, systematic and easy to implement formulation is presented which can be extended to multiloop systems. To avoid the singularity in MATLAB optimization function, a new constraint condition is also introduced in the form of Eq. (25). This condition ensures that the moment of inertia of any link in the linkage system is positive. In the absence of these constraints, an optimization process may lead to solution that is not corresponding to any real linkage.

Acknowledgements

First author acknowledges the scholarship provided by the Government of India under Quality Improvement Program, and the study leave was granted by M.L.V. Textile Institute, Bhilwara (Raj.), India.

Appendix A

A.1. Twist and kinematic constraints

Referring to the planar motion of the ith body, the three-dimensional vector of twist, $\mathbf{t}_i$, is defined as

$$\mathbf{t}_i \equiv \begin{bmatrix} \omega_i \\ \mathbf{v}_i \end{bmatrix} \tag{A.1}$$

where ω_i and $\mathbf{v}_i$ are the scalar angular velocity about the axis is perpendicular to the plane of motion and the two-dimensional vector of linear velocity of the origin of the ith link, O_i, respectively. Note that the twist of the ith body at O_i can be written recursively in terms of the twist of its previous body, #j, at O_j [20] as

$$\mathbf{t}_i = \mathbf{A}_{ij}\mathbf{t}_j + \mathbf{p}_i\dot{\theta}_i \tag{A.2}$$

where the 3×3 twist propagation matrix, $\mathbf{A}_{ij}$, is given by

$$\mathbf{A}_{ij} \equiv \begin{bmatrix} 1 & \mathbf{0}^T \\ \mathbf{E}\mathbf{a}_{ij} & \mathbf{1} \end{bmatrix}, \text{ where } \mathbf{E} \equiv \begin{bmatrix} 0 & -1 \\ 1 & 0 \end{bmatrix} \tag{A.3}$$

Moreover, $\mathbf{a}_{ij}$ is the two-dimensional vector denoting O_j from O_i. Vector $\mathbf{a}_i$ in Fig. 1 implies vector $\mathbf{a}_{i,i+1}$, i.e., $\mathbf{a}_{12} \equiv \mathbf{a}_1$, and so on. Furthermore, the three-dimensional joint-rate propagation vector is given by

$$\mathbf{p}_i \equiv [1 \quad 0 \quad 0]^T, \text{ for revolute joint} \tag{A.4}$$

Also, $\mathbf{1}$ is the 2×2 identity matrix, and $\mathbf{0}$ is the two-dimensional vector of zeros.

Referring to Fig. 1, the links of the four-bar linkage are numbered as #1, ..., #4, where #4 is the fixed link, and the joints are represented as 1, 2, 3, and 4. Position of the mass center of each link is shown by vectors $\mathbf{d}_i$, for $i = 1, 2, 3$, from joints located at O_i. The link lengths are defined by the magnitude of the vectors, $\mathbf{a}_i$, for $i = 1, \ldots, 4$. Since the linkage is opened by cutting joint 3, as shown in Fig. 2, three joint coordinates, θ_i, for $i = 1, 2, 3$, are independent. However, they are not independent for the closed-loop four-bar linkage due to the loop closure constraint. Introducing the nine-dimensional vector of generalized twist, $\mathbf{t} \equiv [\mathbf{t}_1^T, \mathbf{t}_2^T, \mathbf{t}_3^T]^T$, for the open system, it is written using Eq. (A.2) as

$$\mathbf{t} = \mathbf{N}\boldsymbol{\theta}; \text{ where } \mathbf{N} \equiv \mathbf{N}_l\mathbf{N}_d \tag{A.5}$$

In Eq. (A.5) the 9×9 lower block triangular matrix, N_l, and the 9×3 block diagonal matrix, N_d, are given by

$$\mathbf{N}_l \equiv \begin{bmatrix} \mathbf{1} & \mathbf{0} & \mathbf{0} \\ \mathbf{A}_{21} & \mathbf{1} & \mathbf{0} \\ \mathbf{0} & \mathbf{0} & \mathbf{1} \end{bmatrix} \text{ and } \mathbf{N}_d \equiv \begin{bmatrix} \mathbf{p}_1 & \mathbf{0} & \mathbf{0} \\ \mathbf{0} & \mathbf{p}_2 & \mathbf{0} \\ \mathbf{0} & \mathbf{0} & \mathbf{p}_3 \end{bmatrix} \tag{A.6}$$

The matrices $\mathbf{N}_l$ and $\mathbf{N}_d$ are the decoupled natural orthogonal matrices, as introduced in [20] for the open-loop systems whereas the 9×3 matrix, $\mathbf{N}$, is called the natural orthogonal complement (NOC) matrix [21]. Using the expressions of $\mathbf{N}_l$ and $\mathbf{N}_d$, the matrix, $\mathbf{N}$, can be written as

$$\mathbf{N} \equiv \begin{bmatrix} \mathbf{p}_1 & \mathbf{0} & \mathbf{0} \\ \mathbf{A}_{21}\mathbf{p}_1 & \mathbf{p}_2 & \mathbf{0} \\ \mathbf{0} & \mathbf{0} & \mathbf{p}_3 \end{bmatrix} \tag{A.7}$$

In Eq. (A.5), $\boldsymbol{\theta} \equiv [\theta_1, \theta_2, \theta_3]^T$ which is defined as the three-dimensional vector of generalized joint angles, whereas the 3×3 matrix, $\mathbf{A}_{21}$, and the three-dimensional vectors, $\mathbf{p}_1$, $\mathbf{p}_2$ and $\mathbf{p}_3$, are defined in accordance to Eqs. (A.3) and (A.4), respectively.

A.2. Wrench and equation of motion

Similar to the definition of the twist, $\mathbf{t}_i$ of Eq. (A.1), the three-dimensional wrench, $\mathbf{w}_i$, associated with origin of the ith body, O_i, is defined as

$$\mathbf{w}_i \equiv \begin{bmatrix} n_i \\ \mathbf{f}_i \end{bmatrix} \tag{A.8}$$

where n_i and $\mathbf{f}_i$ are the moment about, O_i, and the two-dimensional force at O_i, respectively. From the free-body diagram of the ith body, the Newton–Euler (NE) equations of motion can be expressed as [22,23]

$$I_i^c \dot{\omega}_i = n_i^c \tag{A.9}$$
$$m_i \dot{\mathbf{v}}_i^c = \mathbf{f}_i^c \tag{A.10}$$

where n_i^c is the resultant moment about the mass center, $\mathbf{C}_i$, and $\mathbf{f}_i^c$ is the resultant force acting at $\mathbf{C}_i$. Moreover, m_i and I_i^c are the mass and the inertia of the ith body about C_i, respectively. Since all the kinematic relations are defined with respect to the origin of the moving body, O_i, the NE equations of motion, Eqs. (A.9) and (A.10), are modified accordingly. For this purpose, the velocity and acceleration are transformed about the origin of the body, O_i, as

$$\mathbf{v}_i = \mathbf{v}_i^c - \omega_i \mathbf{E}\mathbf{d}_i \tag{A.11}$$
$$\dot{\mathbf{v}}_i = \dot{\mathbf{v}}_i^c - \dot{\omega}_i \mathbf{E}\mathbf{d}_i + \omega_i^2 \mathbf{d}_i \tag{A.12}$$

Accordingly, the resultant moment and force, n_i and $\mathbf{f}_i$, of the ith body with respect to O_i are expressed as

$$I_i \dot{\omega}_i - m_i \mathbf{d}_i^T \mathbf{E} \dot{\mathbf{v}}_i = n_i \tag{A.13}$$
$$m_i \dot{\mathbf{v}}_i + m_i \dot{\omega}_i \mathbf{E}\mathbf{d}_i - m_i \omega_i^2 \mathbf{d}_i = \mathbf{f}_i \tag{A.14}$$

Eqs. (A.12) and (A.13) are written in compact form as

$$\mathbf{M}_i \dot{\mathbf{t}}_i + \mathbf{C}_i \mathbf{t}_i = \mathbf{w}_i \tag{A.15}$$

where the 3×3 matrices, $\mathbf{M}_i$ and $\mathbf{C}_i$, are as follows:

$$\mathbf{M}_i \equiv \begin{bmatrix} I_i & -m_i \mathbf{d}_i^T \mathbf{E} \\ m_i \mathbf{E}\mathbf{d}_i & m_i \mathbf{1} \end{bmatrix} \text{ and } \mathbf{C}_i \equiv \begin{bmatrix} 0 & \mathbf{0}^T \\ -m_i \omega_i \mathbf{d}_i & \mathbf{O} \end{bmatrix} \tag{A.16}$$

In which $\mathbf{O}$ is the 2×2 matrix of zeros, $\mathbf{0}$ is the two-dimensional vector of zeros, and the 2×2 matrix $\mathbf{E}$ is defined in Eq. (A.3).

Eqs. (A.1)–(A.16) defined for the planar system can be easily extended to spatial system as well. The Newton–Euler (NE) equations of motion for the ith rigid body moving in the three-dimensional Cartesian space with respect to the origin, O_i, are given by [25,26]

$$\mathbf{M}_i\dot{\mathbf{t}}_i + \mathbf{W}_i\mathbf{M}_i\mathbf{E}_i\mathbf{t}_i = \mathbf{w}_i \quad \text{(A.17)}$$

where the 6×6 matrices of the extended mass, $\mathbf{M}_i$, and of the extended angular velocity, $\mathbf{W}_i$, and the 6×6 coupling matrix, $\mathbf{E}_i$ are follows:

$$\mathbf{M}_i \equiv \begin{bmatrix} \mathbf{I}_i & m_i\mathbf{D}_i \\ -m_i\mathbf{D}_i & m_i\mathbf{1} \end{bmatrix}; \quad \mathbf{W}_i \equiv \begin{bmatrix} \boldsymbol{\Omega}_i & \mathbf{O} \\ \mathbf{O} & \boldsymbol{\Omega}_i \end{bmatrix}; \text{ and } \mathbf{E}_i \equiv \begin{bmatrix} \mathbf{1} & \mathbf{O} \\ \mathbf{O} & \mathbf{O} \end{bmatrix} \quad \text{(A.18)}$$

in which $\mathbf{D}_i$ and $\boldsymbol{\Omega}_i$ are the 3×3 cross-product tensors associated with the three-dimensional vectors, $\mathbf{d}_i$ and $\boldsymbol{\omega}_i$, respectively, i.e., $\mathbf{D}_i\mathbf{x} \equiv \mathbf{d}_i \times \mathbf{x}$ and $\boldsymbol{\Omega}_i\mathbf{x} \equiv \boldsymbol{\omega}_i \times \mathbf{x}$, for any three-dimensional Cartesian vector, $\mathbf{x}$. Moreover, $\mathbf{I}_i$ is the 3×3 inertia tensor about the origin, O_i, and $\mathbf{1}$ and $\mathbf{O}$ are the 3×3 identity and zeros matrices, respectively. Furthermore, the six-dimensional vectors of twist, $\mathbf{t}_i$, and wrench, $\mathbf{w}_i$ are defined as

$$\mathbf{t}_i \equiv \begin{bmatrix} \boldsymbol{\omega}_i \\ \mathbf{v}_i \end{bmatrix}, \text{ and } \mathbf{w}_i \equiv \begin{bmatrix} \mathbf{n}_i \\ \mathbf{f}_i \end{bmatrix} \quad \text{(A.19)}$$

where the three-dimensional vectors, $\boldsymbol{\omega}_i$ and $\mathbf{v}_i$, are the angular and linear velocities of the origin, O_i, respectively. Vectors $\mathbf{n}_i$ and $\mathbf{f}_i$ are accordingly the resultant moment about O_i and the resultant force at O_i, respectively.

Appendix B

B.1. Dynamically equivalent systems

The dynamically equivalent system of a body moving in a plane and space require at least two and four mass points, respectively [28,29]. As shown in Fig. 6, consider a frame of reference, $O_iX_iY_iZ_i$, fixed at any arbitrary point, O_i, to the ith rigid body moving in plane or space. A set of n ($\geqslant 2$, for planar and $\geqslant 4$, for spatial motion) point-masses, m_{ij}, are rigidly fixed to the frame of reference at the coordinates (x_{ij}, y_{ij}, z_{ij}) whose $j = 1,\ldots,n$. The point masses are dynamically equivalent to the ith body moving in a plane if following conditions are satisfied:

$$\sum_{j=1}^{n} m_{ij} = m_i \quad \text{(B.1)}$$

$$\sum_{j=1}^{n} m_{ij}x_{ij} = m_i\bar{x}_i; \quad \sum_{j=1}^{n} m_{ij}y_{ij} = m_i\bar{y}_i \quad \text{(B.2–B.3)}$$

$$\sum_{j=1}^{n} m_{ij}(x_{ij}^2 + y_{ij}^2) = I_i^c + m_i d_i^2 \quad \text{(B.4)}$$

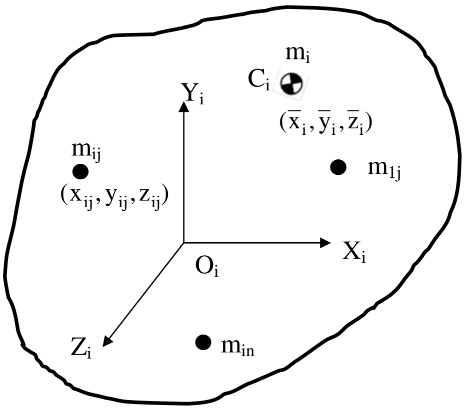

Fig. 6. Dynamic equivalence for a rigid body.

Similarly, the dynamic equivalent system of point-masses for a body moving in a space requires total of 10 conditions, i.e.,

$$\sum_{j=1}^{n} m_{ij} = m_i \tag{B.5}$$

$$\sum_{j=1}^{n} m_{ij}x_{ij} = m_i\bar{x}_i; \quad \sum_{j=1}^{n} m_{ij}y_{ij} = m_i\bar{y}_i; \quad \sum_{j=1}^{n} m_{ij}z_{ij} = m_i\bar{z}_i \tag{B.6–B.8}$$

$$\sum_{j=1}^{n} m_{ij}x_{ij}y_{ij} = I_{i,xy}; \quad \sum_{j=1}^{n} m_{ij}y_{ij}z_{ij} = I_{i,yz}; \quad \sum_{j=1}^{n} m_{ij}z_{ij}x_{ij} = I_{i,zx} \tag{B.9–B.11}$$

$$\sum_{i=1}^{n} m_{ij}(y_{ij}^2 + z_{ij}^2) = I_{i,xx}; \quad \sum_{j=1}^{n} m_{ij}(z_{ij}^2 + x_{ij}^2) = I_{i,yy}; \quad \sum_{j=1}^{n} m_{ij}(x_{ij}^2 + y_{ij}^2) = I_{i,zz} \tag{B.12–B.14}$$

where m_i is the mass, and $(\bar{x}_i, \bar{y}_i, \bar{z}_i)$ are the coordinates of the centre of mass, C_i, of the ith body, whereas $I_{i,xx}$, $I_{i,yy}$, $I_{i,zz}$, $I_{i,xy}$, $I_{i,yz}$ and $I_{i,zx}$ are the elements of the inertia tensor about point O_i of the body with respect to the body fixed frame, $O_iX_iY_iZ_i$. Eqs. (B.5)–(B.14) ensure the same mass, the same centre of mass, and the same inertia ellipsoid of the set of point masses as that of the original body [28,29]. Having defined the dynamically equivalent point-masses for rigid link of a mechanism, dynamic equations of motion for the complete mechanism can be derived in the parameters of the point-masses. These parameters can then be treated as the design parameters to redistribute the link masses for balancing of the mechanism.

References

[1] A.A. Sherwood, B.A. Hockey, The optimization of mass distribution in mechanisms using dynamically similar systems, Journal of Mechanisms 4 (1968) 243–260.

[2] R.S. Berkof, G.G. Lowen, Theory of shaking moment optimization of forced-balanced four-bar linkages, ASME Journal of Engineering for Industry 93B (1) (1971) 53–60.

[3] R.S. Berkof, The input torque in linkage, Mechanism and Machine Theory 14 (1979) 61–73.

[4] G.G. Lowen, F.R. Tepper, R.S. Berkof, The quantitative influence of complete force balancing on the forces and moments of certain families of four-bar linkages, Mechanism and Machine Theory 9 (1974) 299–323.

[5] G.G. Lowen, F.R. Tepper, R.S. Berkof, Balancing of linkages-an update, Mechanism and Machine Theory 18 (3) (1983) 213–220.

[6] K. Ogawa, H. Funabashi, On the balancing of the fluctuation of input torques caused by inertia forces in the crank-and-rocker mechanisms, ASME Journal of Engineering for Industry 91 (1) (1969) 97–102.

[7] B.A. Hockey, The minimization of the fluctuation of input-shaft torque in plane mechanisms, Mechanism and Machine Theory 7 (1972) 335–346.

[8] J.L. Elliott, D. Tesar, The theory of torque, shaking force, and shaking moment balancing of four link mechanisms, ASME Journal of Engineering for Industry 99 (3) (1977) 715–722.

[9] V.H. Arakelian, M.R. Smith, Complete shaking force and shaking moment balancing of linkages, Mechanism and Machine Theory 34 (1999) 1141–1153.

[10] J.L. Wiederrich, B. Roth, Momentum balancing of four-bar linkages, ASME Journal of Engineering for Industry 98 (4) (1976) 1285–1289.

[11] W.L. Carson, J.M. Stephenes, Feasible parameter design spaces for force and root-mean-square moment balancing an in-line 4R 4-bar synthesized for kinematic criteria, Mechanism and Machine Theory 13 (1978) 649–658.

[12] G.G. Lowen, R.S. Berkof, Determination of forced-balance four-bar linkages with optimum shaking moment characteristics, ASME Journal of Engineering for Industry 93 (1) (1971) 39–46.

[13] T.W. Lee, C. Cheng, Optimum balancing of combined shaking force, shaking moment, and torque fluctuations in high speed linkages, ASME Journal of Mechanisms, Transmissions, and Automation in Design 106 (1984) 242–251.

[14] N.M. Qi, E. Pennestrí, Optimum balancing of four-bar linkages, Mechanism and Machine Theory 26 (3) (1991) 337–348.

[15] S.J. Tricamo, G.G. Lowen, A novel method for prescribing the maximum shaking force of a four-bar linkage with flexibility in counterweight design, ASME Journal of Mechanisms, Transmissions, and Automation in Design 105 (1983) 511–519.

[16] S.J. Tricamo, G.G. Lowen, Simultaneous optimization of dynamic reactions of a four-bar linkage with prescribing the maximum shaking, ASME Journal of Mechanisms Transmissions and Automation in Design 105 (1983) 520–525.

[17] Z. Ye, M.R. Smith, Complete balancing of planar linkages by an equivalent method, Mechanism and Machine Theory 29 (5) (1994) 701–712.

[18] I.S. Koshav, General Theory of complete shaking moment balancing of planar linkages: a critical review, Mechanism and Machine Theory 35 (2000) 1501–1514.

[19] H.S. Yan, R.C. Soong, Kinematic and dynamic design of four-bar linkages by links counterweighing with variable input speed, Mechanism and Machine Theory 36 (2001) 1051–1071.
[20] S.K. Saha, Dynamics of serial multibody systems using the decoupled natural orthogonal complement matrices, ASME Journal of Applied Mechanics 66 (1999) 986–996.
[21] J. Angeles, S. Lee, The formulation of dynamical equations of holonomic mechanical systems using a natural orthogonal complement, ASME Journal of Applied Mechanics 55 (1988) 243–244.
[22] P.E. Nikravesh, Computer-aided Analysis of Mechanical Systems, Prentice Hall, Englewood Cliffs, New Jersey, 1988.
[23] A.A. Shabana, Computational Dynamics, John Wiley & Sons, Inc., New York, 1994.
[24] MATLAB , Version 7.0.0.19920 (R14), May 06, 2004.
[25] H. Chaudhary, S.K. Saha, Matrix formulation of constraint wrenches for serial manipulators, International Conference on Robotics and Automation (ICRA 2005), Barcelona, Spain, April 18–22, 2005, pp. 4647–4652.
[26] S.K. Saha, J. Angeles, The formulation of kinematic constraints in design-oriented machine dynamics, ASME International Conference on Advances in Design Automation 2 (1991) 115–122.
[27] G. Strang, Linear Algebra and its Applications, Harcourt, Brace, Jovanovich, Publisher, Florida, 1998.
[28] E.J. Routh, Treatise on the Dynamics of a System of Rigid Bodies, Elementary Part I, Dover Publication Inc., New York, 1905, 3–28.
[29] R.A. Wenglarz, A.A. Forarasy, L. Maunder, Simplified Dynamic Models, Engineering 208 (1969) 194–195.
[30] P.E. Nikravesh, Systematic reduction of multibody equations of motion to a minimal set, International Journal of Non-linear Mechanics 25 (2/3) (1990) 143–151.
[31] P.E. Nikravesh, G. Gim, Systematic construction of the equations of motion for multibody systems containing closed kinematic loops, Journal of Mechanical Design 115 (1993) 143–149.